JOTCS A Journal of the Turkish Chemical Society Section: A Chemistry

TURKISH CHEMICAL SOCIETY

Equilibrium and Kinetic Studies of a Cationic Dye Adsorption onto Raw Clay

Eda GÖKIRMAK SÖĞÜT[1*], Necla ÇALIŞKAN KILIÇ[2]

[1] *Van Security Vocational School*
[2] *Department of Physical Chemistry Faculty of Science, Van Yüzüncü Yıl University, 65080 Van, Turkey*

Abstract: In this study, methylene blue (MB) dye adsorption from the aqueous solution on raw clay samples collected from the Tilkitepe in the east of Lake Van was presented. Batch adsorption studies were conducted to evaluate the effect of various experimental parameters such as pH, contact time and initial concentrations on the removal of MB. The five nonlinear adsorption equations were applied to describe the equilibrium isotherms. Considering the correlation coefficients, the order of the most suitable isotherm models was Sips> Freundlich> Temkin> Dubinin- Radushkevich>Langmuir. From the data applied to the pseudo-first-second order, Elovich and intra-particle diffusion kinetic models, it can be said that the best model describing the kinetics of MB dye adsorption is the pseudo-second order (PSO) kinetic model. The results are shown that Tilkitepe / Van raw clay material could be used as an economical and effective adsorbent for dye removal.

Keywords: Methylene blue, raw clay, adsorption, kinetic models, non-linear isotherms.

Submitted: December 10, 2019. **Accepted:** July 09, 2020.

Cite this: GÖKIRMAK SÖĞÜT E, ÇALIŞKAN KILIÇ, N. Equilibrium and Kinetic Studies of a Cationic Dye Adsorption onto Raw Clay. JOTCSA. 2020;7(3):713–26.

DOI: https://doi.org/10.18596/jotcsa.657621.

***Corresponding author.** E-mail: edagokirmak@yyu.edu.tr.

INTRODUCTION

The rapid development of technology caused many industries to release their wastes into the environment without subjecting them to a pre-cleaning process. Dyes and pigment industries often produce waste containing organic matter and high color (1). Nowadays, synthetic dyes are used more in the industry because of their low-cost production, stability, and color diversity compared to natural dyes. When these pigments are released into the environment, they damage the ecology in the soil and water they contact with sunlight. Therefore, the removal of industrial wastes containing dye emerges as one of the most critical aims in environmental studies. There are more than 100.000 kinds of dye, which are classified as anionic and cationic. The cationic dyes contain protonated amine or sulfur-containing groups and have a net positive charge (2).

MB dye is not accepted among toxic dyes but has harmful effects on living organisms and is used in the coloring of many materials. It is also used as the determination of surface properties, oxidation-reduction indicator, pesticide industries, antiseptic, and for other medical purposes (3-5). Therefore, an effective method is required to remove the dye from the

wastewater. Some methods, such as chemical precipitation (6), ion-exchange (7), adsorption (8), membrane technologies (9), and photocatalysis (10), are used in the removal process. Adsorption is the most widely known and used; it is quite remarkable because it provides ease of design and use (11).

Generally, porous materials such as clay, chitin, peat, silica, and activated carbon have been used for the adsorption of heavy metals and dyes from aqueous solution (12). Some adsorbents are not economical due to regeneration problems. Also, the cost of production and other parameters such as regeneration, usability, environmental compatibility, and the energy consumption is essential in the selection of adsorbents (13). For this reason, the related studies aim to find a more economical and effective sorbent when compared to activated carbon (12). Due to their advantageous physicochemical characteristics such as high surface area, high cation exchange capacity, and layer structure, clays are known to be highly capable of removing waste from aqueous solution (14, 15). Balancing the negatively charged layers with the hydrated cations placed in the intermediate layers is an important feature of the clays (14).

In recent years, many scientific studies have centered on the investigation of locally available clay as low-cost adsorbents**.** Van lake basin is rich in some industrial raw materials. The people of the region use clayey soils in the region for personal cleaning practices and the production of pottery since ancient ages. There are no studies other than the structural characterization of the clayey soil in the region and the determination of its adsorption capacity of heavy metals (16). It is imperative to determine the chemical, physicochemical and adsorptive properties of the materials that can be used as an industrial raw material in the region and to use the raw material without pretreatment without energy expenditure and secondary chemical waste. The adsorption of organic molecules onto clay is affected by its surface characteristics and the chemical properties of the molecules (15). Due to the high affinity of cationic dye molecules for clay surfaces, they are readily adsorbed by treated with clay suspensions (14).

This study aimed to evaluate the potential of Tilkitepe natural clay as a low-cost adsorbent to remove methylene blue from the aqueous solution as an ideal alternative to the expensive methods available for removing dyes from wastewater. The natural adsorbent was characterized by XRF, XRD, and FT-IR techniques. The batch experiments were applied to understand the nature of the adsorption of MB dye from the aqueous solution onto natural clay. The effects of initial dye concentration, contact time, temperature, and pH on adsorption were investigated to emphasize the importance of optimum conditions in determining the nature of adsorption. The obtained data were enforced to several isotherm models, kinetic models, and the advantages of natural material in waste dye removal were presented.

MATERIALS AND METHODS

Adsorbent

The natural clay samples were collected from the Tilkitepe/Van region was powdered in a mortar. No pretreatment has been applied to the material. After passing through a 230 mesh sieve (62.0 μm), it was stored in the polymer bags and denoted as TM.

Adsorbate

Methylene blue (MB, MF:$C_{16}H_{18}N_3SCl$ and MW: 319.852 g) was obtained from Merck. The dye's chemical structure is showed in Figure 1 and a stock solution (1000 mg L^{-1}) was prepared and then diluted with distilled water at different concentrations.

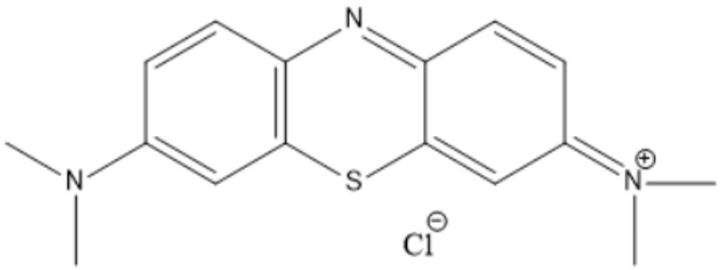

Figure 1. The chemical structure of methylene blue.

Characterization of the Sample

Chemical analysis of the Tilkitepe raw clay was made using the Philips 2400 XRF instrument. XRD analysis was obtained using an X-ray diffractometer (Philips PW 1830-40) with Ni-filtered Cu X-ray tube devices at 2-40 degrees. FT-IR analysis was performed before and after the adsorption process, using a Thermo Scientific Nicolet S10 FT-IR spectrometer with wavenumber range from 400 to 4000 cm^{-1} (16).

Methods

The adsorption experiments were applied at ambient temperature with a solution of 0.1 g of adsorbent in 10 mL of an aqueous solution of several concentrations of the dye (10, 20, 30, 45, and 60 mg L^{-1}). The effect of pH was investigated using HCl and NaOH solutions (pHs 2, 3, 4, 5, 6, 7, 8, 9). These measurements were made using a WTW pH meter (Series 720, Germany). The batch adsorption process was carried out using a heat-controlled shaker with a constant agitation speed of 125 rpm at 298 K. The samples were filtered, and the residual concentrations of MB in the filtrate were measured to learn about the final concentration of MB dye by using a UV / Vis Spectrophotometer (PG Instruments T80) at 664 nm. The amounts of dye adsorbed by the adsorbent and the adsorption efficiency (%) were calculated from using the following equation (17).

$$q_e = \frac{(C_0 - C_e)V}{m} \quad (1)$$

$$\%Adsorption = \frac{C_0 - C_e}{C_0} \times 100 \quad (2)$$

Where, C_0 (mg L^{-1}) is the initial liquid phase concentration, and C_e (mg L^{-1}) is equilibrium liquid-phase concentrations of the dye, q_e (mg g^{-1}) represents the amount of dye adsorbed, V (L) is the volume of the solution, and m (g) is the mass of the adsorbent used.

Adsorption Isotherms

Langmuir, Freundlich, Dubinin-Radushkevich, Temkin, and Sips and non-linear isotherms were used to explain the nature of the Methylene blue adsorption on the natural adsorbent (surface properties, mechanism of adsorption). The isotherm parameters were determined by non-linear regression analysis (with Originlab. 17). The C_e-q_e values obtained for dye adsorption on the natural adsorbent were applied to each non-linear isotherm equation. For each isotherm model, standard errors (S.E) were also calculated to determine the isotherm that best fits the experimental data. Besides, a chi-square value (χ^2), which is a statistical data required for the suitability of the obtained adsorption system, was calculated using the same software (16, 18). The non-linear regression method, which was applied in the computerized process, that minimizes the error distribution between the experimental data and the estimated isotherms, was applied (19).

These parameters are determined in the following Eq.3 and 4 (20).

$$R^2 = \frac{\Sigma(q_{e,calc} - \overline{q_{e,exp}})^2}{\Sigma(q_{e,calc} - \overline{q_{e,exp}})^2 + \Sigma(q_{e,calc} - q_{e,exp})^2} \quad (3)$$

$$\chi^2 = \sum_{i=1}^{N} \frac{(q_{e,exp} - q_{e,calc})^2}{q_{e,calc}} \quad (4)$$

where $q_{e,calc}$ (mg g^{-1}) is calculated from the isotherm for corresponding $q_{e,exp}$(mg g^{-1}), which is obtained from the batch experiment and $q_{e,exp}$ is the average of $q_{e,\ exp}$. Also, N represents the number of observations in experimental data. The fact that R^2 is close to unity, $\chi 2$, and S.E close to zero is an indicator of the most suitable isotherm model (21)

Langmuir Isotherm

According to the Langmuir isotherm model, there are active adsorption centers on the surface of the sorbent, and they all have equivalent energy. Furthermore, according to this model, the adsorption equilibrium is a dynamic equilibrium and the molecules attached to the surface do not interact with each other (22).

$$q_e = \frac{q_M K_L C_e}{1 + K_L C_e} \quad (5)$$

Where q_m is the maximum adsorption capacity (mg g^{-1}), and K_L is the Langmuir isotherm constant (L g^{-1}).

Freundlich Isotherm

The Freundlich equation is used to describe heterogeneous systems and is expressed in the following equation.

$$q_e = K_F C_e^{1/n} \quad (6)$$

Where K_F is Freundlich isotherm constant (L g^{-1}), and n is the heterogeneity factor in the Freundlich model. If 1 / n value is below unity, it shows normal adsorption, but if 1 / n is above unity, it indicates cooperative adsorption (23).

Dubinin–Radushkevich Isotherm
This isotherm is usually applied by Gaussian energy distribution to express the adsorption mechanism on heterogeneous surfaces.

$$q_e = q_M \exp(-K_{DR}\varepsilon^2)$$
$$\varepsilon = RTln(1+\frac{1}{C_e}) \quad (7), (8)$$

Where K_{DR} is D-R isotherm constant, R is the ideal gas constant (8.314 (J mol^{-1} K^{-1}), and ε is the Polanyi potential.

If the energy value is less 8 kJ mol^{-1}, the physical interactions are in the adsorption. Conversely, if the energy is more than 8 kJ mol^{-1}, the adsorption mechanism can be defined by chemical interactions (24).

Temkin Isotherm
Temkin isotherm model assumes that the adsorption heat (a function of temperature) of all molecules in the layer will decrease linearly (23).

$$q_e = \frac{RT}{b_T}\ln(K_T C_e) \quad (9)$$

where K_T is Temkin isotherm equilibrium binding constant (L g^{-1}),b_T is Temkin isotherm constant (kJ mol^{-1}), R is the ideal gas constant (8.314 (J mol^{-1} K^{-1}), T is the temperature (K).

Sips Isotherm
Sips isotherm model is used to describe adsorption on heterogeneous surfaces. Sips isotherm model is a combination of Langmuir and Freundlich isotherm models. It shows the characteristics of Freundlich isotherm at low concentrations and gives the characteristics of Langmuir isotherm by estimating the monolayer adsorption capacity at high concentrations (21).

$$q_e = \frac{K_S(a_S C_e)^{n_S}}{1+(a_S C_e)^{n_S}} \quad (10)$$

Where K_S is Sips isotherm constant (L g^{-1}), a_S is Sips isotherm constant, (L mg $^{-1}$), and n_S is Sips isotherm exponent.

Kinetics
The pseudo-first-order (PFO) kinetic model is expressed as follows (25).

$$q_t = q_e[1-\exp(-k_1 t)] \quad (11)$$

where k_1 (min^{-1}) is PFO rate constant and t (min) is the contact time.

Y.S. Ho developed the pseudo second order (PSO) kinetic model and was expressed as follows:

$$q_t = \frac{k_2 q_e^2\, t}{1+k_2 q_e t} \quad (12)$$

where k_2 (g mg^{-1} min^{-1}) is PSO rate constant.

The intra-particle diffusion model is as follows:

$$q_t = k_i\, t^{1/2} + C \quad (13)$$

where k_i is the rate constant (mg g^{-1} $min^{-0.5}$)

The Elovich equation, which is representative of the active solid regions being energetically heterogeneous and therefore representing different activation energies for chemical adsorption, interprets the absorption kinetics and is graphed with the following equation.

$$q_t = \frac{1}{\beta}\ln(1+\alpha\beta t) \quad (14)$$

where α (mg g^{-1} min^{-1}) is the initial adsorption rate, β (g mg^{-1}) is the desorption constant related to the extent of surface coverage and activation energy for chemisorption (26).

RESULTS

Surface Properties and Characterization of Adsorbent
Tilkitepe raw clay is composed of SiO_2 37.5%, and it has 20.5% CaO, 6.2% MgO, 5.6% Al_2O_3, 5.4% Fe_2O_3, 0.6% TiO_2, 2.0% Na_2O, 1.3% K_2O, 0.1% MnO and 0.1% P_2O_5. The XRD analysis indicates the predominance of quartz and calcite in the raw clayey material, with the most intense peaks, a low quantity of feldspar, smectite, and illite. The surface properties and characterization of adsorbent, which include

clay minerals and non-clay minerals, are presented in detail in the previous paper (16). The functional groups contributing to the adsorption process were measured, and the FT-IR spectrum of clay adsorbent before and after the adsorption is in the wavenumber range 4,000–400 cm^{-1} and is presented in Figure 2.

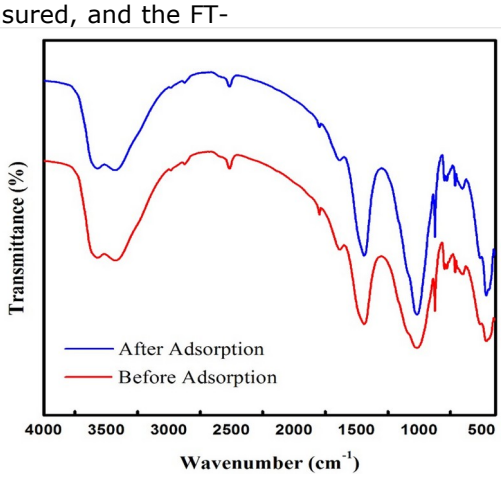

Figure 2. The FTIR spectra of before and after adsorption of methylene blue onto Tilkitepe-originated clayey material.

The two bands at 3568 and 3424 cm^{-1} were ascribed to hydroxyl groups involved in hydrogen bonds (Si–Si-OH or Al–Al–OH), respectively. 2985 and 1436 cm^{-1} peaks indicate the presence of (C – H) group vibrations. The band appearing at 1629 cm^{-1} is due to the H_2O bending vibration. Si-O-Al is bending vibration, 871.82 cm^{-1} attributed to Fe–Al–OH of montmorillonite, and Si-O-Si bending vibrations can be attributed to 509.21 cm^{-1} and 462.92 cm^{-1}, respectively (16). The FTIR spectra of the raw clay and MB adsorbed clay showed that is a noticeable change in intensity of the bands with no change locations. After the adsorption of MB, the density of Si-O-Si (siloxane peak) was increased in 1014 due to the electrostatic attraction between the positive dye cation and the negative clay surface (Figure 2). Furthermore, the band density of the hydroxyl group observed in 3568, and 3424 cm^{-1} (Figure 2) appears to decrease after MB adsorption (27). The changes in the FTIR spectra confirmed that the process involved is type inclusion of methylene blue on the Tilkitepe raw clay (28).

Influence of pH on the Adsorption

The effect of pH on the ability of Tilkitepe raw clay to remove methylene blue (MB) from aqueous solution was investigated. The pH of the solution is one of the most effective parameters in the adsorption process, mainly due to the importance of adsorbents on the surface functional groups and adsorption properties (29). The effect of pH on the adsorption efficiency (%) was calculated using Eq. 2 and presented Figure 3.

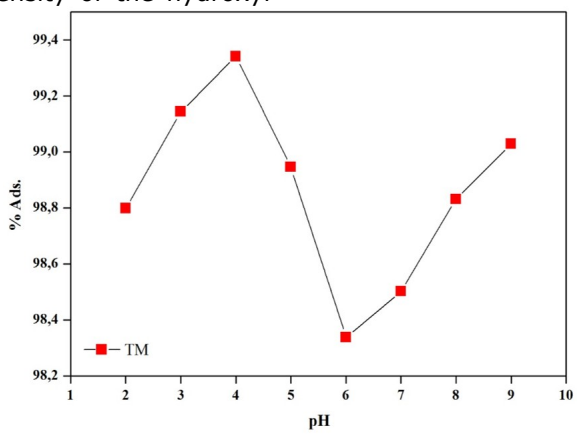

Figure 3. pH effect on the adsorption of methylene blue on raw clay at 30 mg L^{-1} initial solution concentration (298 K).

The pH control was adjusted by adding HCl and NaOH solutions, and the highest adsorption efficiency was achieved as 99.34% at pH = 4. It might be the result of increased protonation by neutralizing negative charges on the adsorbent surface because the cationic dye targets the electron-rich centers (30). It was observed that the amount of dye removal starts to increase again at higher than pH = 7. Alkaline solutions might cause the change in the polarity of the dye, and methylene blue might have demethylated to other conventional dyes. Similar results were presented in other publications (31-33). It indicated that the adsorption capacity of MB onto Tilkitepe in solution was pH-dependent. Therefore, it was decided to perform batch adsorption tests at pH = 4. In substance, Tilkitepe raw clay with a smectic clay density is composed of an octahedral alumina layer between the outer layers of tetrahedral silica. The silanol groups on the clay surface can be said to form a hydrogen bond to an amine group and to form an ionic bond with another amine group Si-O. Besides, in many studies, clay has also been interpreted to interact with dye molecules through hydrogen bonds and hydrophobic-hydrophobic mechanisms (34-36).

Effect of initial dye concentration with contact time

The determination of the effect of the initial ion concentration is critical because it provides the initial repulsive force necessary to get over the mass transfer opposition of the dye through the sol-sorbent interface (37). Fig.4a and b show the effect of the initial dye concentration (10-60 mg L^{-1}) as a function of contact time (1-120 min) at the removal of MB by Tilkitepe clay.

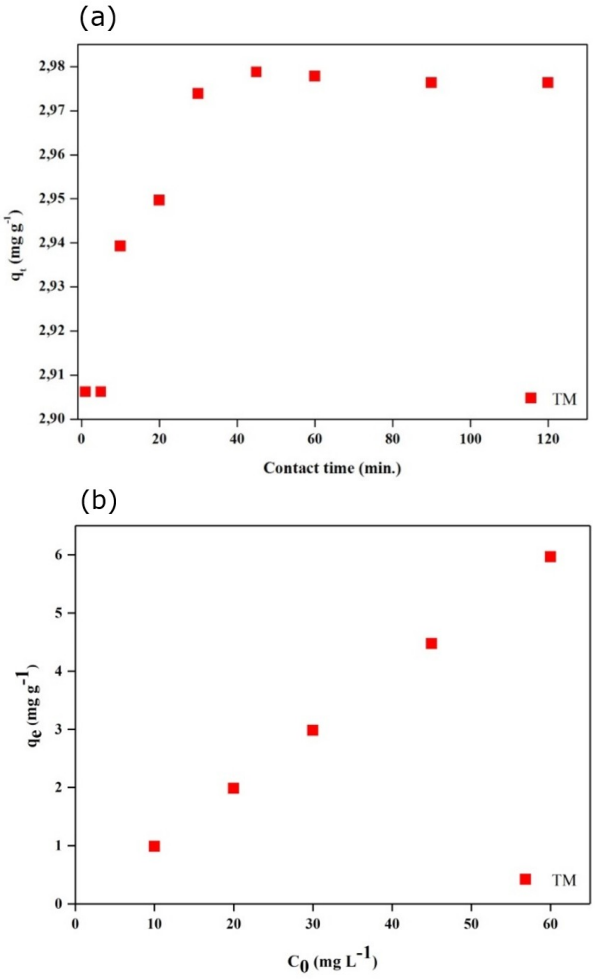

Figure 4. a) Effect of contact time for the adsorption of methylene blue onto Tilkitepe (C_0:30 mg L^{-1}, T: 298 K), b) The effects of the initial solution concentration on the adsorption at 298 K.

With increasing concentration for dye adsorption, as presented in Figures 4.a. and b., the adsorption initially increases. The experiments were decided to be performed for

90 minutes to ensure equilibrium saturation. The first rapid uptake may be for external diffusion of the dye to the adsorbent surface. As time progresses, slower uptake may be attributed to slower intracellular diffusion due to lower dye concentration and constant adsorbent amount in the adsorption system (38).

Adsorption isotherms

The analysis of isotherm results provides essential information, such as the nature of the adsorbent and its surface properties (39). Non-linear diagrams of isotherm models for dye (MB) adsorption on the Tilkitepe raw clay are given in Fig. 5. The values of isotherm models are listed in Table 1.

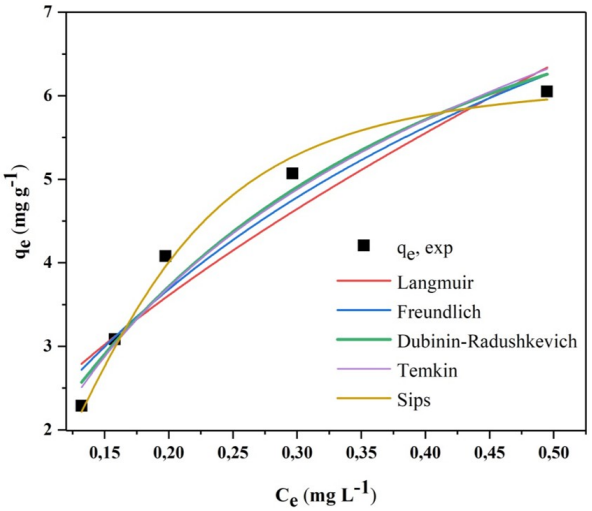

Figure 5. Comparison of adsorption isotherm models for the sorption of methylene blue on Tilkitepe at 298 K.

Table 1. The values of non-linear isotherm models for methylene blue adsorption onto Tilkitepe.

Isotherm/Model		Value	S.E
Langmuir	q_M (mg g^{-1})	11.870	1.2900
	K_L	2.2466	0.1042
	R_L	0.0426	
	R^2	0.9015	
	χ^2	0.2431	
Freundlich	K_F	9.8099	0.2598
	n	1.6098	0.3292
	R^2	0.9590	
	χ^2	0.8942	
Dubinin-Radushkevich	q_M (mg g^{-1})	9.9823	0.8061
	K_{D-R}	0.2623	0.0367
	E_{D-R}	1.3807	
	R^2	0.9350	
	χ^2	0.9512	
Temkin	b_T	0.8602	0.3757
	K_T	18.0560	1.5064
	R^2	0.9355	
	χ^2	0.8741	
Sips	q_M (mg g^{-1})	10.9787	0.3312
	a_S	6.1725	0.2137
	n_S	2.866	0.5234
	R^2	0.9819	
	χ^2	0.9096	

Langmuir isotherm, which accepts monolayer and homogeneous adsorption, can be caused not only by physical interactions but also by powerful electrostatic attractions. The R^2 value determined from the Langmuir equation is 0.9015; the χ^2 value is 0.2431 at 298 K. The q_m

value was determined to be 11.870, and S.E was found to be 1.2900. The R_L values were found to be 0.0426; it can be said that the Langmuir isotherm is favorable for the adsorption (40). However, the Freundlich isotherm model has a higher regression coefficient (0.9590) and lower S.E (0.2598) and χ^2 (0.8942) values. Also, the K_F and n values were calculated as 9.8099 and 1.6098, respectively. If n lies between one and ten, this indicates a favorable sorption process (23). 1/n (0,6211) value between 0 and 1 showed that the natural sorbent easily adsorbed MB. The D-R adsorption isotherm provided useful data for this study (R^2 = 0.9350). It has a lower S.E (0.8061) and χ^2 (0.9512) values. As the adsorption energy (E) values are below 8 kJ mol^{-1} at the studied temperature, thus, it can be said that the adsorption mechanism is a combination of physical adsorption and electrostatic interaction (41). In physical adsorption, adsorbates exhibit relatively low adsorption energies as they adhere to the adsorbent through weak Van der Waals interactions. The low value (0.8602) of the Temkin constant bT (kJ mol-1) obtained from the Temkin Isotherm model also supports a weak adsorbate-adsorbent interaction. The correlation coefficient obtained from Temkin isotherm at 298 K is 0.9355, and lower S.E (0.3757) and χ2 (0.8741) values (20, 42). If n_S = 1, a dimensionless heterogeneity factor in the Sips isotherm equation, this equation is reduced to the Langmuir isotherm equation and indicates that the adsorption process is homogenous (43). This isotherm model has a higher regression coefficient (0.9819) and lower S.E (0.3312) and χ^2 (0.9096) values. It has been verified that adsorption is heterogeneous from the Sips isotherm constant (6.1725) in Table 1.

Adsorption kinetics

Kinetic studies are critical in illuminating the adsorption mechanism. It is known that non-linear kinetic models are more accurate in assigning the correct models to the tested data (44). Different kinetic models such as pseudo-first-order, pseudo-second-order, Elovich non-linear kinetic models, and Weber and Morris intraparticle diffusion model were used in the evaluation of the experimental data in Figure 6. Higher R^2 and lower error function values are referred to as better model fitting. The results of the modeling data for the MB adsorption on the natural adsorbent are presented in Table 2 a-b.

Table 2 a. Pseudo-first and -second-order and Elovich kinetic parameters of Methylene Blue adsorption onto Tilkitepe clay at 30 mg L^{-1} initial dye concentrations (T = 298 K).

Kinetic Models		**Value**	**SE.**
	$q_{e\ (exp)}$ (mg g^{-1})	**2.9778**	-
Pseudo-first order	$q_{e.\ (cal)}$ (mg g^{-1})	0.0075	0.0059
	k_1 (min^{-1})	0.0075	0.0540
	χ^2	0.0024	
	R^2	0.5954	
Pseudo-second order	$q_{e.\ (cal)}$ (mg g^{-1})	2.9797	0.0030
	k_2 (g mg^{-1} min^{-1})	3.6686	0.2404
	X^2	0.0043	
	R^2	0.9502	
Elovich	α (mg g^{-1} min^{-1})	1.2115	10.6052
	β (g mg^{-1})	35.8904	2.9699
	χ^2	0.0176	
	R^2	0.7451	

Table 2 b. Intraparticle diffusion parameters at (30 mg L^{-1} initial dye concentrations and T = 298 K).

Intraparticle Diffusion Model	Tilkitepe clay
	298 (K)
k_{id} (($mg\ g^{-1}h^{1/2}$)	**0.0011**
C_o	2.9326
R^2	0.7871

The pseudo-first-order kinetic model is usually among the applied kinetic models and has an expression based on the adsorption capacity of the adsorbent (Eq. (11)). It is seen that there is a significant difference between the calculated values (qe (calc)) and the experimental values (qe (exp)) from Table 2 a. Compared to other model parameters, lower correlation coefficient values that this model is not applicable for MB adsorption on the natural adsorbent (45).

The pseudo-second-order kinetic model helps predict the adsorption rate of a given adsorption system. The adsorption ratio is based on the assumption that the number of bonding areas on the adsorbent is proportional to the square (46). Equation (Eq.(12)) and corresponding constants are presented in Table 2 a. It is observed that the values of qe (calc) and qe (exp) are almost similar, and χ^2 is at a lower value, and R^2 value is 0.9502. Therefore, the MB adsorption on the natural adsorbent follows the pseudo second-order kinetic model sufficiently (47).

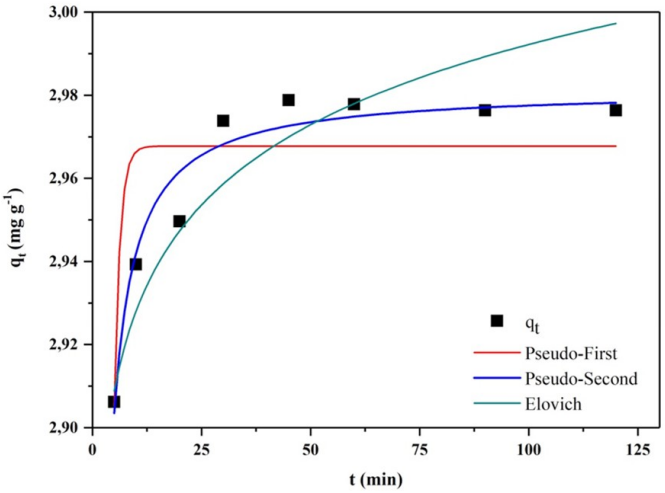

Figure 6. Non-linear kinetic model of pseudo-first-order, pseudo-second-order, and Elovich models for Methylene blue adsorption onto Tilkitepe at 298 K.

The Elovich model, a kinetic model, based on adsorption capacity, assumes that the adsorption mechanism is chemical or physical adsorption (48). The Elovich equation (Eq. (14)) and the characteristic parameter values are presented in Table 2 a, respectively. Table 2 shows the applicability of this model in that the value of χ^2 is significantly lower at 298 K. The low values of the correlation coefficients at the temperature discuss the suitability of this model for the experimental data (49).

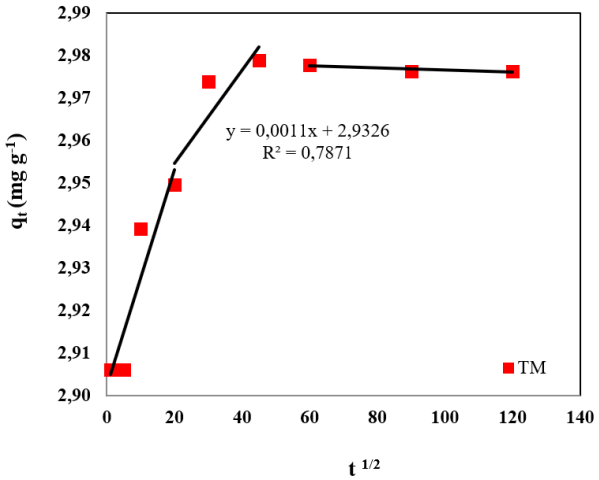

Figure 7. Intraparticle diffusion plots for adsorption (C_0= 30 mg L^{-1} and T = 298 K).

The intra-particle diffusion plot was calculated with Eq. 13 and presented in Figure 7. If the particle diffusion was involved in the adsorption process, the plot would appear a straight line,

and if the rate-limiting step were only particle diffusion, this line would pass through the origin (50). It is evident in Figure 7 that there are three separate stages in each case. i) The first stage with high slope represents the fastest process, mass or surface diffusion; ii) the second stage is slower than the first stage, which shows the effect of pore diffusion or intra-particle diffusion controlled region; iii) the last stage is almost linear and indicates the equilibrium state of the system (51). As can be seen, the plot did not pass through the origin; thus it can be said that intra-particle diffusion is not the only rate-limiting step in the adsorption process (52) The boundary layer thickness of the calculated diffusion coefficient is listed in Table 2 b.

CONCLUSION

The raw Tilkitepe clay is an excellent alternative adsorbent to remove the MB dye from the aqueous solutions. When this adsorbent is suspended in water, it interacts with the dye at the solid/liquid interface. The dye molecules in the structure of clay form active areas by hydrating in aqueous solution depending on pH. Thus, MB is attracted to negatively charged surfaces of clay or interlamellar can be replaced with cations in space; the charge density is pH-dependent (38). Equilibrium isotherm modeling of MB adsorption was performed, and the data best fit the Freundlich and Sips isotherm models. Among the most critical kinetic models evaluated in the adsorption mechanism, the pseudo-second kinetic (PSO) model is the most suitable model. Furthermore, the intra-particle diffusion model has linear regions, and it is proposed that multiple adsorption rates can follow adsorption. The maximum capacity (q_M) of this adsorbent, which is cheap and does not cause secondary pollution, was determined as 11.870 mg g^{-1} from the experimental data.

REFERENCES

1. Chakraborty S, Chowdhury S, Das P. Artificial neural network (ANN) modeling of dynamic adsorption of crystal violet from aqueous solution using citric-acid-modified rice (Oryza sativa) straw as adsorbent. Clean Technologies and Environmental Policy. 2012;15:doi: 10.1007/s10098-012.

2. Errais E, Duplay J, Darragi F, M'Rabet I, Aubert A, Huber F, et al. Efficient anionic dye adsorption on natural untreated clay: Kinetic study and thermodynamic parameters. Desalination. 2011;275(1):74-81.

3. Deng H, Lu J, Li G, Zhang G, Wang X. Adsorption of methylene blue on adsorbent materials produced from cotton stalk. Chemical Engineering Journal. 2011;172(1):326-34.

4. Chunjiaozhou, Zhenwu, Wenjiezhang, Mingxiaxia, Guozhangdai, Guangmingzeng, et al. FACILE SYNTHESIS OF HUMIC ACID-COATED IRON OXIDE NANOPARTICLES AND THEIR APPLICATIONS IN WASTEWATER TREATMENT. Functional Materials Letters. 2012;04.

5. Mouni L, Belkhiri L, Bollinger J-C, Bouzaza A, Assadi A, Tirri A, et al. Removal of Methylene Blue from aqueous solutions by adsorption on Kaolin: Kinetic and equilibrium studies. Applied Clay Science. 2018;153:38-45.

6. Alvarez MT, Crespo C, Mattiasson B. Precipitation of Zn(II), Cu(II) and Pb(II) at bench-scale using biogenic hydrogen sulfide from the utilization of volatile fatty acids. Chemosphere. 2007;66(9):1677-83.

7. Wong C-W, Barford JP, Chen G, McKay G. Kinetics and equilibrium studies for the removal of cadmium ions by ion exchange resin. Journal of Environmental Chemical Engineering. 2014;2(1):698-707.

8. Sadhukhan B, Mondal N, Chattoraj S. Biosorptive removal of cationic dye from aqueous system: A response surface methodological approach. Clean Technologies and Environmental Policy. 2013;16.

9. Qiu Y-R, Mao L-J. Removal of heavy metal ions from aqueous solution by ultrafiltration assisted with copolymer of maleic acid and acrylic acid. Desalination. 2013;329:78-85.

10. Gupta VK, Jain R, Nayak A, Agarwal S, Shrivastava M. Removal of the hazardous dye—Tartrazine by photodegradation on titanium dioxide surface. Materials Science and Engineering: C. 2011;31(5):1062-7.

11. Shen Z, Jin F, Wang F, McMillan O, Al-Tabbaa A. Sorption of lead by Salisbury biochar produced from British broadleaf hardwood. Bioresource technology. 2015;193:553-6.

12. Afroze S, Sen T, Ang H, Nishioka H. Adsorption of methylene blue dye from aqueous solution by novel biomass Eucalyptus sheathiana bark: equilibrium, kinetics,

thermodynamics and mechanism. Desalination and Water Treatment. 2015;57:1-21.

13. Mondal N, Das K, Das B, Sadhukhan B. Effective utilization of calcareous soil towards the removal of methylene blue from aqueous solution. Clean Technologies and Environmental Policy. 2015;18:1-17.

14. Gürses A, Doğar Ç, Yalçın M, Açıkyıldız M, Bayrak R, Karaca S. The adsorption kinetics of the cationic dye, methylene blue, onto clay. Journal of Hazardous Materials. 2006;131(1):217-28.

15. Fatiha M, Belkacem B. Adsorption of methylene blue from aqueous solutions using natural clay. Journal of Materials and Environmental Science. 2016;7(1):285-92.

16. Caliskana N, Sogutb EG, Savrana A, Kula AR, Kubilaya S. Removal of Cu (II) and Cd (II) ions from aqueous solutions using local raw material as adsorbent: a study in binary systems. DESALINATION AND WATER TREATMENT. 2017;75:132-47.

17. Ertaş M, Acemioğlu B, Alma MH, Usta M. Removal of methylene blue from aqueous solution using cotton stalk, cotton waste and cotton dust. Journal of Hazardous Materials. 2010;183(1):421-7.

18. Foo KY, Hameed BH. Insights into the modeling of adsorption isotherm systems. Chemical Engineering Journal. 2010;156(1):2-10.

19. Salarirad MM, Behnamfard A, editors. Modeling of equilibrium data for free cyanide adsorption onto activated carbon by linear and non-linear regression methods. International Conference on Environment and Industrial Innovation; 2011.

20. Rahman M, Sathasivam KV. Heavy metal adsorption onto Kappaphycus sp. from aqueous solutions: the use of error functions for validation of isotherm and kinetics models. BioMed research international. 2015;2015.

21. Samarghandi M, Hadi M, Moayedi S, BARJESTEH AF. Two-parameter isotherms of methyl orange sorption by pinecone derived activated carbon. 2009.

22. Wong YC, Szeto YS, Cheung WH, McKay G. Equilibrium Studies for Acid Dye Adsorption onto Chitosan. Langmuir. 2003;19(19):7888-94.

23. A.O D, Olalekan A, Olatunya A, Dada AO. Langmuir, Freundlich, Temkin and Dubinin–Radushkevich Isotherms Studies of Equilibrium Sorption of Zn 2+ Unto Phosphoric Acid Modified Rice Husk. J Appl Chem. 2012;3:38-45.

24. Ho Y. Adsorption of heavy metals from waste streams by peat, University of Birmingham, Birmingham, UK Ph. D: Thesis; 1995.

25. Al-Musawi TJ, Brouers F, Zarrabi M. Kinetic modeling of antibiotic adsorption onto different nanomaterials using the Brouers–Sotolongo fractal equation. Environmental Science and Pollution Research. 2017;24(4):4048-57.

26. Ahmad MA, Ahmad Puad NA, Bello OS. Kinetic, equilibrium and thermodynamic studies of synthetic dye removal using pomegranate peel activated carbon prepared by microwave-induced KOH activation. Water Resources and Industry. 2014;6:18-35.

27. Mohamed EA, Selim AQ, Zayed AM, Komarneni S, Mobarak M, Seliem MK. Enhancing adsorption capacity of Egyptian diatomaceous earth by thermo-chemical purification: Methylene blue uptake. Journal of Colloid and Interface Science. 2019;534:408-19.

28. Tarik A, Abdelmjid A, Kabbaj M, Elkouali M, Bennamara A, Charrouf M, et al. Valorization of natural clay from agadir (Morocco): Characterization and study of the isotherms adsorption of Methylene blue. Journal of Chemical and Pharmaceutical Research. 2014;6:599-606.

29. Feddal I, Ramdani A, Taleb S, Gaigneaux EM, Batis N, Ghaffour N. Adsorption capacity of methylene blue, an organic pollutant, by montmorillonite clay. Desalination and Water Treatment. 2014;52(13-15):2654-61.

30. Shahryari Z, Soltani Goharrizi A, Azadi M. Experimental study of methylene blue adsorption from aqueous solutions onto carbon nano tubes. Int J Water Resour Environ Eng. 2010;2.

31. Nsami N, Mbadcam J. The Adsorption Efficiency of Chemically Prepared Activated Carbon from Cola Nut Shells by ZnCl2 on

Methylene Blue. Journal of Chemistry. 2013;2013.

32. Goyal M, Singh S, Bansal R. Equilibrium and Dynamic Adsorption of Methylene Blue from Aqueous Solutions by Surface Modified Activated Carbons. Carbon letters. 2004;5.

33. Gottipati R, Susmita M. Aplication of Biowaste (Waste Generated in Biodiesel Plant) as an Adsorbent for the Removal of Hazardous Dye – Methylene Blue from Aqueous Phase. Brazilian Journal of Chemical Engineering. 2010;27:357-67.

34. Al-Degs YS, El-Barghouthi MI, El-Sheikh AH, Walker GM. Effect of solution pH, ionic strength, and temperature on adsorption behavior of reactive dyes on activated carbon. Dyes and Pigments. 2008;77(1):16-23.

35. Mukherjee K, Kedia A, Korukonda JR, Dhir S, Paria S. Adsorption Enhancement of Methylene Blue Dye at Kaolinite Clay – Water Interface Influenced by Electrolyte Solutions. RSC Advances. 2015;5.

36. Fang Y, Zhou A, Yang W, Araya T, Huang Y, Zhao P, et al. Complex Formation via Hydrogen bonding between Rhodamine B and Montmorillonite in Aqueous Solution. Scientific Reports. 2018;8.

37. Patil S, Renukdas S, Patel N. Removal of methylene blue, a basic dye from aqueous solutions by adsorption using teak tree (Tectona grandis) bark powder. International Journal of Environmental Sciences. 2011;1:711-26.

38. Tong Ks, Azraa A, Noordin M. Isotherms and Kinetics Studies on the Removal of Methylene Blue from Aqueous Solution by Gambir. International Journal of Environmental Science and Development. 2012:232-6.

39. Feddal I, Ramdani A, Taleb S, Gaigneaux E, Batis N, Ghaffour N. Adsorption capacity of methylene blue, an organic pollutant, by montmorillonite clay. Desalination and water treatment. 2013;52:1–8.

40. Tan IAW, Ahmad AL, Hameed BH. Adsorption of basic dye on high-surface-area activated carbon prepared from coconut husk: Equilibrium, kinetic and thermodynamic studies. Journal of Hazardous Materials. 2008;154(1):337-46.

41. Caliskan N, Kul AR, Alkan S, Sogut EG, Alacabey İ. Adsorption of Zinc(II) on diatomite and manganese-oxide-modified diatomite: A kinetic and equilibrium study. Journal of Hazardous Materials. 2011;193:27-36.

42. Araújo CST, Almeida ILS, Rezende HC, Marcionilio SMLO, Léon JJL, de Matos TN. Elucidation of mechanism involved in adsorption of Pb(II) onto lobeira fruit (Solanum lycocarpum) using Langmuir, Freundlich and Temkin isotherms. Microchemical Journal. 2018;137:348-54.

43. Nethaji S, Sivasamy A, Mandal A. Adsorption isotherms, kinetics and mechanism for the adsorption of cationic and anionic dyes onto carbonaceous particles prepared from Juglans regia shell biomass. International Journal of Environmental Science and Technology. 2013;10(2):231-42.

44. Bujdák J. Adsorption kinetics models in clay systems. The critical analysis of pseudo-second order mechanism. Applied Clay Science. 2020;191:105630.

45. Ponnusamy SK, K K. Equilibrium and Kinetic Study of Adsorption of Nickel from Aqueous Solution onto Bael Tree Leaf Powder. Journal of Engineering Science and Technology. 2009;4.

46. Plazinski W, Dziuba J, Rudzinski W. Modeling of sorption kinetics: The pseudo-second order equation and the sorbate intraparticle diffusivity. Adsorption. 2013;19.

47. Aljeboree AM, Alshirifi AN, Alkaim AF. Kinetics and equilibrium study for the adsorption of textile dyes on coconut shell activated carbon. Arabian Journal of Chemistry. 2017;10:S3381-S93.

48. Cestari AR, Vieira EF, Matos JD, dos Anjos DS. Determination of kinetic parameters of Cu (II) interaction with chemically modified thin chitosan membranes. Journal of Colloid and Interface Science. 2005;285(1):288-95.

49. Vilvanathan S, Shanthakumar S. Ni(2+) and Co(2+) adsorption using Tectona grandis biochar: kinetics, equilibrium and desorption studies. Environmental technology. 2018;39(4):464-78.

50. Zhang L, Loaiciga H, Xu M, Du C, Du Y. Kinetics and Mechanisms of Phosphorus Adsorption in Soils from Diverse Ecological Zones in the Source Area of a Drinking-Water

Reservoir. International Journal of Environmental Research and Public Health. 2015;12:14312-26.

51. Biswas S, Sen T, Yeneneh A, Meikap B. Synthesis and characterization of a novel Ca-alginate-biochar composite as efficient zinc (Zn 2+) adsorbent: Thermodynamics, process design, mass transfer and isotherm modeling. Separation Science and Technology. 2018:1-19.

52. Inyinbor AA, Adekola FA, Olatunji GA. Kinetics, isotherms and thermodynamic modeling of liquid phase adsorption of Rhodamine B dye onto Raphia hookerie fruit epicarp. Water Resources and Industry. 2016;15:14-27.